

# We are IntechOpen, the world's leading publisher of Open Access books Built by scientists, for scientists

6,900

Open access books available

186,000

International authors and editors

200M

Downloads

Our authors are among the

154

Countries delivered to

TOP 1%

most cited scientists

12.2%

Contributors from top 500 universities



WEB OF SCIENCE™

Selection of our books indexed in the Book Citation Index  
in Web of Science™ Core Collection (BKCI)

Interested in publishing with us?  
Contact [book.department@intechopen.com](mailto:book.department@intechopen.com)

Numbers displayed above are based on latest data collected.  
For more information visit [www.intechopen.com](http://www.intechopen.com)



---

# Elastomer Application in Microsystem and Microfluidics

---

Shuang (Jake) Yang and Kunqiang Jiang

Additional information is available at the end of the chapter

<http://dx.doi.org/10.5772/48121>

---

## 1. Introduction

Elastomer has been widely used in academic and industry since it was invented in the nineteenth century <sup>1</sup>. By definition, elastomer is a polymer which is viscoelastic and able to regain its shape after deformation. Compared to other materials, elastomer has notably low Young's modulus and high yield strain. In general, amorphous elastomer is made of carbon, hydrogen, oxygen and/or silicon whose glass transition temperature is well below the application temperature, e.g., room temperature. As a result, it has excellent properties in elasticity <sup>2</sup>, transparency <sup>3</sup>, permeability <sup>4</sup>, and insulation <sup>5</sup>.

One of the most commonly used elastomers is silicone elastomer such as poly(dimethylsiloxane) (PDMS), which has been widely used in electronics and microfluidics due to its elasticity, optical transparency, UV transmission, permeability, biocompatibility, and availability. PDMS generally consists of repeat unit dimethylsiloxane. The repeat methyl is modifiable using functional groups such as urea or bis-urea for development of high mechanical strength of elastomer. The modified PDMS presents both a high mechanical strength and elasticity at room temperature due to functionality of the cross-linking domains and intrinsic reversibility of the supramolecular chains. PDMS is optically transparent and is usually inert, non-toxic and non-flammable <sup>6</sup>. PDMS is viscoelastic and is normally measured using dynamic mechanical analysis (DMA), in which a specialized instrument is used to determine the material's flow characteristics over a wide range of temperature, flow rates, and deformations. In general, the shear modulus of PDMS is in the range of 100 kPa to 3 MPa, varied with the preparation conditions.

Characterization of elastomer by dynamic-mechanical testing includes temperature sweep, frequency sweep, strain sweep, damping and friction properties. The dynamic mechanical measurement is particularly useful to characterize conductive particles in elastomer for

understanding the particles effect on overall elastomer mechanical properties. It is very common to measure damping factor ( $\tan \delta$ ) change with temperature for understanding the elastomer degree of crosslinking<sup>7</sup>. The dynamic mechanical testing provides information on both uncrosslinked and crosslinked phases of the elastomer, as well as viscoelasticity. To this end, nanoindentation plays a significant role on viscoelastic characterization of elastomers for their creep and relaxation properties<sup>8,9</sup>.

Elastomer is an excellent matrix which can mix with other materials such as conductive particles and thermoplastics to enhance mechanical properties. For example, silver particles are added into silicone elastomer matrix to formation of conductive elastomer for high-density electrical contacts in microelectronics. Polypropylene and ethylene-propylene copolymer elastomer significantly improves the dynamic mechanical, tensile and impact properties and even changes the modes of failure<sup>10</sup>. The size, shape and spatial packing of elastomer inclusions are the most significant factors in controlling the mechanical behavior of blends. Since PDMS can be cured with different ratio of dimethylsiloxane and curing reagent, it is very useful to fabricate microfluidic devices for a variety of applications, including cell culture<sup>11</sup>, ELISA assay<sup>12</sup>, capillary electrophoresis<sup>13</sup>, DNA sequencing<sup>14</sup>.

In this chapter, we briefly discussed elastomer elastic and viscoelastic properties, as well as permeability. Elastomer is widely used in microelectronics and microfluidics due to all or part of these characteristics. Then we discussed several applications in microelectronics and microfluidics using elastomer as substrate. Finally, we introduce potential development of elastomer.

## 2. Elastomer property and its applications

Elasticity is the ability of a material to return to its original shape and size after being stretched, compressed, twisted or bent<sup>15</sup>. Elastic deformation (change of shape or size) lasts only as long as a deforming force is applied to the object, and disappears once the applied force is removed. The elasticity of elastomer makes it extremely useful in microelectronics and microfluidics. For example, the Intel CPU uses land grid array sockets (LGA), in which the socket has over thousands of elastomer contacts that consist of silver particles in elastomer matrix<sup>16,17</sup>. When socket, the CPU and printed circuit board (PCB) are assembled by compressing force, the silver-embedded elastomer is compressed to increase contact area between socket and the CPU, and between socket and the PCB. The excellent elastic deformation of elastomer can keep the electrically tight contact for minimum contact resistance. Elasticity of PDMS minimizes its stress relaxation and creep effect, which is severe in other polymer with low elasticity. The excellent elasticity of PDMS allows to release from microfluidic masters without damaging PDMS device<sup>18,19</sup> and significant deflection to occur when a pressure difference develops<sup>20</sup>. Therefore, it is important to characterize PDMS elasticity and understand how to improve such property for various applications.

The most common elasticity experiment for many decades involved mechanically blending a reinforcing filler such as carbon black into natural rubber, crosslinking the elastomer with sulfur, and characterizing its network structure by stress-strain measurements in simple

extension, or by extents of equilibrium swelling<sup>21</sup>. However, in most instances, such as thin-film elastomer, land grid array elastomer contact, and PDMS microfluidics, these methods may not be applicable due to effects of supporting materials. To characterize elastomer in those applications, nanoindentation has been an emerging technology for elastomer characterization and is an indispensable tool in many instances where other techniques are inapplicable. Nanoindentation is such tool for characterization of polymer on its viscoelasticity. Indentation technique was first introduced as advent of indentation fracture mechanics<sup>22</sup> in 1975 and ever since it has been developed for characterization of elastic-plastic materials using the Oliver-Pharr's method<sup>23</sup>. No valid method was reported for polymer nanoindentation analysis based on stress-strain experiments until the viscoelastic model was proposed in 2004 and other emerging studies that followed<sup>8, 24, 25</sup>. Because of viscoelasticity, elastic-plastic model cannot be directly used to derive modulus and hardness. Also these measurements are dependent on the experimental parameters, such as loading rate, maximum load, holding duration, unloading rate, and minimum unloading force<sup>26</sup>. To minimize the effects by those experimental parameters during indentation, the experimental conditions were proposed in such a way that fast loading was applied for minimizing viscoelastic deformation, long dwell time for full viscoelastic deformation, and quick unloading rate. The fast loading and unloading showed that only elastic-plastic deformation was observed, while viscoelastic deformation was observed in the dwell duration. Also, it was observed that the viscoelastic deformation can be measured by keeping a minimum force on the indenter so that the instrument can record the deformation progress with time. The modulus and viscosity coefficient of elastomer can be derived using flat-ended punch-tip<sup>8</sup>, the elastic-viscoelastic-viscous deformation is described by following equation,

$$h = \frac{P_0 h_{in}}{E_0 A_0} + \sum_1^n \frac{P_0 h_{in}}{E_i A_0} (1 - e^{-E_i t / \eta_i}) + \frac{h_{in}}{\eta_o} t$$

where  $P$  represents load,  $h$  is deformation and subscript  $e$  is elastic,  $\eta$  coefficient of viscosity,  $E$  modulus,  $t$  time. Elastic modulus is thus derived by  $P_0 h_{in} / A_0 h_e$ . This model provides a means for characterization of elastomer, such as investigation of effect of crosslinking, work of adhesion and fluid environment on elastic modulus<sup>24</sup>. Nanoindentation on PDMS indicated that it is capable of measuring several order of magnitudes of elastic modulus of PDMS, with expected increase of the elastic modulus at higher crosslinked PDMS (2.80 MPa at 10:1 ratio, and 0.88 MPa at 30:1 ratio; monomer:crosslinker, wt%)<sup>24, 27</sup>.

Elastomer is permeable to solvents, gases, moisture or even some small molecules<sup>4, 28-30</sup>. Permeability has been employed to fabricate non-contact pump for the manipulation of aqueous solutions within PDMS microfluidic devices<sup>20</sup> or supply oxygen for large-scale culture of hepatocytes<sup>31</sup>. On the other hand, PDMS permeability limits its application to microfluidic technology, in which coating such as glass-like layer using sol-gel chemistry is developed on PDMS to minimize permeability<sup>32</sup>. The permeability of a PDMS film or membrane to a penetrant (i.e., gas or solvent) is defined as<sup>28, 33</sup>,

$$P_A = \frac{N_A l}{p_{2A} - p_{1A}}$$

Where  $P_A$  is the permeability coefficient,  $N_A$  is the steady-state penetrant flux through the film,  $p_{1A}$  and  $p_{2A}$  are the downstream and upstream partial pressures of component  $A$ , and  $l$  is the membrane or film thickness. In general, PDMS permeability depends strongly on the feeding gas/solvent composition and temperature: an increase in vapor concentration or liquid pressure leads to increased chain mobility at constant feeding pressure and temperature, resulting in high diffusivity and permeability. The increase of permeability with pressure is attributed to the swelling of PDMS.

Due to the permeability nature of PDMS, many researchers synthesized co-polymer which contained PDMS as a permeable medium for gas/solvent. For example, the 'smart' tri-component amphiphilic membranes consisting of poly(ethylene glycol) (PEG), PDMS and poly(pentamethylcyclopentasiloxane) (PD5) domains were synthesized for biological applications, including immunoisolation of cells<sup>29, 30</sup>. The high oxygen permeability of PDMS makes it feasible for the application in microdevices in cell culture<sup>34</sup>. Compared to large-scale system / platform, microfluidics provides suitable environments for sample interaction, such as cell culture, with the significant increase of surface-to-volume ratio while the fluidic behavior is similar to the environments in vivo<sup>29</sup>. Integration of PDMS into microfluidic platform can implement studies on cell-to-cell interactions and understanding of cell behaviors in vitro, emulation of situations observed in vivo. Several studies have demonstrated that microfluidic devices consisted of two PDMS layers were capable for cell culture<sup>35</sup>. They further fabricated a complex microfluidics which consisted of stacking ten PDMS layers, in which four cell culture chambers and one-oxygen chamber inserts between.

### 3. Elastomer as electrical contact matrix in microelectronics

Insulation elastomer in microelectronics plays a significant role to prevent a short-circuit<sup>36</sup>. Electrical insulating polymers have been introduced nearly one hundred years ago and proved to be excellent long-term physical and electrical properties, including weatherability, moisture-sealing, corrosion resistant and durability. The polymer insulating materials are used in a wide range of applications such as surge arresters, insulators, insulation enhancement, and bushings<sup>5</sup>. The initial polymers used in insulating materials were mainly on radiation-crosslinked and semicrystalline polyolefin copolymers. With development of manufacturing and materials technologies, elastomer has been increasingly designed for insulating applications<sup>5, 37</sup>.

The elastomer formulations have been optimized so that an exceptional electrical and weathering performance is achieved, which are equal or above that of polyolefin copolymer materials. The silicone elastomer has many advantages such as hydrophobicity, hydrophobic recovery, weathering resistance, processability, and elastomeric mechanical properties. These advantages make silicone elastomer suitable for outdoor insulating applications. For example, PDMS has been used for high-voltage (HV) outdoor insulation in the real world as a replacement over conventional porcelain and glass insulation. As one silicone elastomer, PDMS as HV insulating materials is light weight, has superior vandal resistance, and contains better contamination performance. However, many research works

have been conducted on molecular modification in order to improve PDMS properties, including degradation under exposure to discharge and arcing, mechanical strength etc. It has been demonstrated that hydrophobicity of PDMS can be rendered by exposure to discharges, which can be recovered when exposure ceases. Their studies showed that the lowly crosslinked PDMS can readily reorient between hydrophilic and hydrophobic states, therefore improving its weathering capabilities<sup>38</sup>.

Recently, PDMS has been micropatterned using a photoresist lift-off technique for selective electrical insulation in microelectrode array applications<sup>39</sup>. The micropatterning technique is able to manufacture PDMS patterns with feature as small as 15  $\mu\text{m}$  and various thicknesses down to 6  $\mu\text{m}$ . With micropatterned PDMS insulation layer, the electrical resistance between adjacent electrodes is within the specification. Additionally, the micropatterned PDMS insulation can be applied to biosensing microdevices such as in an extensive neuronal network. Other researchers used PDMS to develop a replaceable insulator for a single-use planar microelectrode array (MEA) in the study of electrogenic tissues<sup>40</sup>. They demonstrated applications using microstencils for rejuvenation of an old MEA and the fabrication of a single-use MEA.

Conductive materials are used to produce shielding gaskets for military, aerospace, electronics, and communications. The conductive elastomers are designed to balance requirements for electrical conductivity, thermal management, and cost performance<sup>41</sup>. Conductive elastomer materials are ideal for customer applications requiring both excellent electromagnetic interference shielding and environmental sealing across a wide range of temperature. The conductive elastomers could be blended polyacetylene with different types of thermoplastic elastomers: styrene-butadiene-styrene, styrene-isoprene-styrene, and styrene-ethylenebutylene-styrene tri-block copolymers<sup>42</sup>. The polyacetylene is a highly conjugated polymer which contains high concentration of unsaturated sites. Those sites are easily attacked by ozone / UV light and reacted with elastomer, formation of conductive elastomer composites. Or insulation elastomers are coated with compliant electrode material on both sides of the elastomer film<sup>43</sup>. The dielectric elastomers were actuated by means of electrostatic forces applied via compliant electrodes. The performance of conductive elastomers is dependent on many factors, e.g., elastomer crosslinking method and type of monomer. In an electrically conductive heterogeneous binary polymer blends, consisting of ethylene-propylene-diene-monomer (EPDM) and polyaniline (PAni), the performance was significantly affected by the crosslinking method<sup>44</sup>. In the blend, PAni underwent doping upon exposure to a protonic acid and became electrically conductive. Several methods have been studied for monomer crosslinking, such as the use of a phenolic resin for unsaturated rubbers and high service temperature products, inter-chain C-C bonds formation after the reticulation reaction, electron beam induced crosslinking for 3-D network. Results indicated that electron beam irradiation crosslinking method was not affected by the presence of the acid necessary for doping the conductive elastomers.

Insulation elastomer has been used as a matrix to hold conductive particles in land grid array socket since it significantly improves contact resistance and increases interconnect density. The need for high density electronics has led to the development of semiconductor

array packages, such as ball grid array (BGA) and land grid array (LGA) packages. However, soldering a package to a printed circuit board (PCB) is challenging for input/output (I/O) counts greater than a thousand, and solder joint defects can induce reliability problems in the application. These problems can be solved by using an LGA socket, which eliminates the soldering process, provides a separable interconnect between the component and the PCB, and also enables easy product rework, repair, and upgrade. The conductive particles in elastomer matrix has been introduced into electronics in 1980's<sup>16, 45</sup>. One such conductive elastomer composite is called Z-direction anisotropically conductive materials which are made of the magnetic alignment of conductive particles in elastomers<sup>46</sup>. The composites contain many vertically aligned but laterally isolated chains of ferromagnetic metal spheres, and the ends of which protrude from the surfaces for better electrical contact. These materials exhibit Z-direction only electrical conduction, in combination with the compliant nature of the materials, can be exploited advantageously for a variety of electronic applications, including fine-pitch, area-array, circuit interconnects, circuit-testing, heat sink interfacing, and sensor devices<sup>47, 48</sup>. The schematic diagram of this design structure is shown in Figure 1. This design has been used in a tactile shear sensor for applications such as robotic skins or grippers, touch sensitive actuators, and finger operated controls<sup>49</sup>.

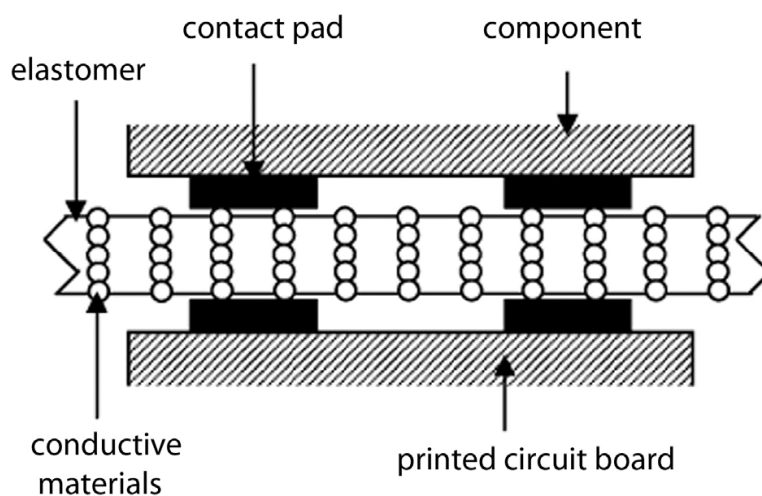


**Figure 1.** Schematic diagram of a Z-direction only electrical conduction, in which the component is electrical connected to the printed circuit board through vertically aligned and laterally isolated conductive materials. The contact is made by external contact force. Reprint and permission from<sup>16</sup>

An LGA socket assembly consists of component, socket, and board as shown in Figure 2. The contact force is applied through a fixture<sup>16, 45</sup>. The socket design can vary in terms of target component, contact, and housing. One class of LGA sockets incorporates conductive particles in elastomer (polymer) as electrical interconnects for LGA. This class of socket has comparatively low cost, ease of assembly, and short signal path; the elastomer has a sealing effect. However, elastomer-based interconnection is susceptible to failure due to creep and stress relaxation, whenever a force or deformation is provided. A decrease in the contact force due to stress relaxation may lead to the degradation of contact resistance. Increase of

elasticity can effectively mitigate creep and stress relaxation, in that crosslinked elastomer has instantaneous recovery after removal of stress.

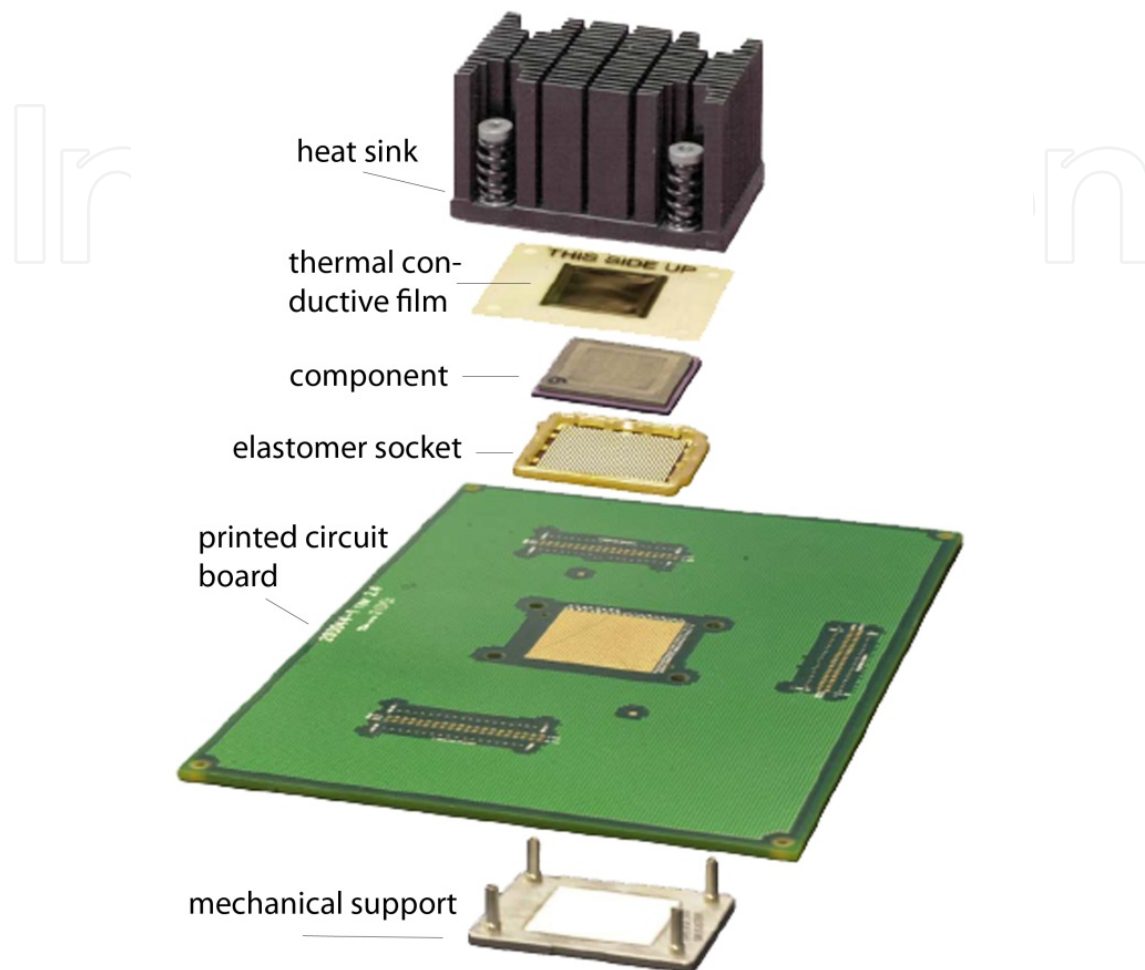


**Figure 2.** Schematic diagram of elastomer land grid socket assembly. The interconnection part, elastomer socket, can be replaced with different type of sockets, including metalized particle interconnect (MPI), PariPoser film, and conductive rubber sockets (CRS). Reprint and permission from <sup>16</sup>

Several mechanisms can lead to the elastomer failure, such as electrochemical migration <sup>50-52</sup>, stress relaxation and creep <sup>45, 53</sup> and corrosion <sup>16</sup>. This section will extensively emphasize these mechanisms and use respective models to predict the lifecycle of the components. The metal electrochemical migration was first identified in the short-circuit failure of Sun Microsystems Sun Fire 6800. Investigation on the failed parts did not observe any dendrite to bridge adjacent components and/or contacts. In general, dendrites were considered to short the electrical circuit. This finding indicated that even without dendrite formation a short-circuit can happen. The design of the experiment, which mimicked the device environment with accelerated conditions, was conducted to identify the failure mechanism and electrochemical migration processes based on the failure products <sup>50-52</sup>. The new failure mechanism in the metal-in-elastomer socket was proposed on the facts that surface insulation resistance has catastrophically decreased and unknown materials were formed on

surface after a certain period of time incubation in the temperature-humidity-bias conditions. The metal-in-elastomer socket consists of silver particles in elastomer matrix. Previous studies showed that silver can migrate in the humidity-temperature-bias conditions<sup>54</sup>. However, those studies added the external conductive ions, e.g., contaminants or silver ions, into the system to initialize the migration process<sup>55</sup>. In recent studies, several substantial results exploited different electrochemical migration, including silver electrochemical migration (ECM) processes, migration products, and failure criterion on surface insulation resistance ( $10^5$  ohm).

The silver ECM could occur when bias was applied to silver-in-elastomer socket in the humidity-temperature. Initially, the water layer absorbed on the surface is electrolyzed to hydrogen and hydroxide ions, which further migrate to cathode and anode respectively. Silver oxides to silver ions by accepting electrons through electrolyzed water solution under bias, and silver ions are accumulated in absorbed water layer. The silver ions are also migrated to cathode through water layer. Overall, the surface insulation resistance (SIR) decreases when ions are generated in the absorbed water layer, or formation of conductive electrolyte. The short-circuit failure occurs when silver ion concentration increases to the specific value when the surface insulation resistance decreases to  $10^5$  ohm.

Both film and dendrites were observed on the film after permanent failure when the surface insulation resistance of the silver-in-elastomer was less than 1000 ohm. Studies on this regard showed that the film growth was developed in deionized water, while the dendrite growth was developed in high conductivity water. It was found that the film grew on the surface without distinctive direction while dendrites grew from cathode to anode. The analysis of film and dendrites from electron scanning spectrometry and X-ray photoelectron microscopy showed that the film consists of silver oxide and dendrites are silver only. The process of the silver electrochemical migration is progressed as follow: silver oxidation at anode to formation of silver ion; silver ion migration from anode to cathode through absorbed water layer (6-7 water monolayers); partial silver ion reduction to silver oxide with hydroxide from water electrolysis (film); other silver ion reduction to formation of silver at the cathode (dendrites)<sup>50-52</sup>.

New failure criterion on surface insulation resistance was proposed. In the IPC standard (IPC-TR-476A), the failure was defined as the surface insulation resistance below  $10^6$  ohm. New experimental findings showed that the component didn't fail when resistance below the resistance, no electrochemical migration related products detected either<sup>50-52</sup>. In addition, the surface insulation resistance immediately decreased to the order of  $10^6$  ohm when the metal-in-elastomer was conditioned in the highly accelerated stress testing ( $130^\circ\text{C}/85\% \text{RH}/\text{bias}$ ). Until SIR was below  $10^5$  ohm, the silver dendrites were observed. The resistance ultimately was within hundreds of ohms when the dendrites bridged the adjacent contacts.

The new ECM process was proposed as: presence of moisture, anodic metal dissolution or ion generation and ion migration to cathode (electrochemical reaction), ion accumulation, and metal dendritic growth. The ion accumulation was found to be the rate controlling step

in which the surface insulation resistance degraded significantly when the ion concentration accumulated to a specific value. This added step explained the failure occurrence without dendritic formation/bridging and perfected the process. Time-to-failure (TTF) model considered these factors to estimate the failure time, including water adsorption, ion generation, ion migration, and ion accumulation. The dendritic growth was excluded from the model based on the experimental findings. Furthermore, incorporation of dendritic growth model with TTF model can be used to estimate time-to-permanent component failure, since the dendritic bridge creates a permanent conductive path between conductors.

The ion-accumulation based model assumed that the silver discharged at the anode was directly proportional to the amount of electrical charge that passed through the electrode, or Faraday's Law, the total mass of metal dissolution equaled the total mass of metal ions discharged into the electrolyte. Unlike the bulk resistance of conductive particles in elastomer<sup>56</sup>, by use of Ohm's law and Brunauer-Emmett-Teller (BET) model<sup>57</sup>, the time-to-failure model was given by,

$$TTF = nF \times \frac{m_0}{M} \times \beta \times \frac{1}{V} \times \frac{(1 - RH)[1 + (c - 1)RH]}{cRH} \times e^{\left(\frac{E_\sigma}{RT}\right)}$$

Where  $\sigma_s$  is the surface insulation conductivity,  $R$  is the resistance,  $m_0$  is the critical mass loss required to dissolve to reach the critical ion concentration when resistance decreases to value of failure criterion,  $V$  is potential,  $RH$  is relative humidity,  $n$  is chemical valence,  $M$  is the molecular weight,  $F$  and  $R$  are constant,  $\beta$ ,  $c$  and  $E_\sigma$  are coefficient relevant to relative humidity, temperature and materials properties. Using this model, the time-to-failure is estimated for elastomer sockets. For silver in elastomer socket, the  $TTF$  can be simplified as,

$$TTF = 1.11 \times 10^{-5} \times \frac{1}{V} \times \frac{(1 - RH)}{RH} \times e^{\left(\frac{7846}{T}\right)}$$

Based on this model, the silver-in-elastomer socket fails in 150 hours after incubation in 90°C/90%/20 V conditions; while it can resist up to 27000 h in service at conditions of 25°C/50%/110 V.

Another failure mechanism is called creep and stress relaxation due to viscoelastic elastomer as matrix in socket. As shown in Figure 2, the mechanical support fixed elastomer deformation as constant. As a result, the stress applied to the socket is expected to decrease gradually due to the stress relaxation of elastomer. To understand failure mechanism and its effect on contact resistance, the dynamic mechanical analyzer (DMA) was used to characterize elastomer stress relaxation. The chamber of DMA can control temperature by air gas and liquid nitrogen. Creep is performed by constant stress and stress relaxation by constant strain. The creep process is often categorized into three stages: primary creep (a stage of decreasing creep rate), secondary creep (a stage of constant creep rate), and tertiary creep (a stage of increasing creep rate). When the load is initially applied, there is an instantaneous elongation, a primary stage of a transient nature during which slip and work hardening occur in the most favorably oriented grains. Then there is a secondary stage of steady-state creep during which the deformation continues at an approximately constant rate. The third stage (tertiary stage) takes place when the stress is high enough that the creep

rate accelerates until fracture occurs<sup>58</sup>. The results for the creep of the silicone elastomer are shown in Figure 3 (a). Both primary and secondary creeps are observed. The results show that the creep deformation increases with temperature. The constant creep rate during the secondary stage was also a function of temperature.

Stress relaxation refers to the time-dependent contact force decrease under a constant strain. Figure 3 (b) plotted behavior of stress relaxation of elastomer under various temperatures. The significance of stress relaxation on elastomer socket is that contact resistance increases at a decreased contact force. It is thus important to derive the relationship time-dependent contact resistance due to stress relaxation of elastomer. Combination of stress relaxation and contact resistance, the time-dependent contact resistance model is derived<sup>45</sup>,

$$R_c = \frac{\rho}{2} \sqrt{\frac{\pi H}{F_0[1 - B \ln(\frac{t}{C} + 1)]}} + \frac{\sigma_f H}{F_0[1 - B \ln(\frac{t}{C} + 1)]}$$

Where the  $R_c$  is contact resistance,  $\rho$  is electrical resistivity (ohm.m),  $H$  is contact hardness,  $F_0$  is initial contact force,  $t$  is time, and  $B, C$  are temperature dependent parameters, given by,

$$B = 1.20 \times 10^{-4}T, \text{ and } C = 6.62 \times 10^{-7}T e^{\frac{1130}{T}} \text{ (for silicon elastomer)}$$

The  $R_c - t$  can be used for estimation of contact resistance degradation of metal-in-elastomer socket for scheduled socket replacement.

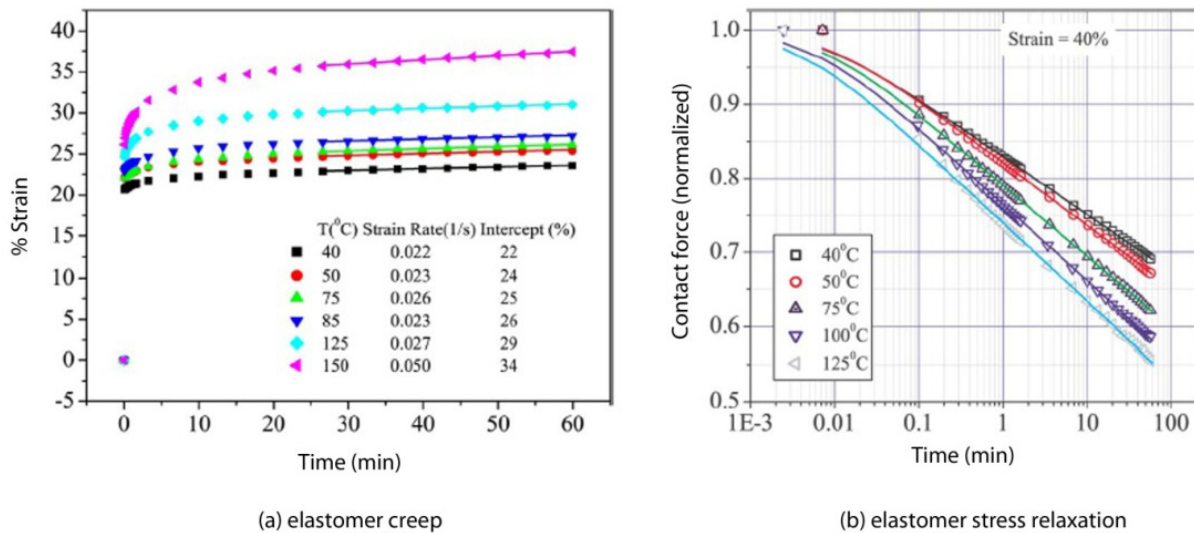


**Figure 3.** Elastomer creep (a) and stress relaxation (b) behavior at various temperatures. Dots: experimental data; solid line: fitted curve. Reprint and permission from<sup>45</sup>

#### 4. Elastomer as substrate in microfluidics

Elastomer is also one of popular materials for microfluidics application as substrate, micro-valves, pumps<sup>59-61</sup>. Elastomer can be easily patterned by curing on a micromachining mold as an alternative microfabrication technique. The soft lithography technique, which

generates micropatterns by contact printing and microstructures by embossing and replica molding, has been used to manufacture blazed grating optics, stamps for chemical patterning, and microfluidics devices<sup>19, 62, 63</sup>. Different from photolithography technique<sup>64</sup>, the soft lithography is not subject to the limitations set by optical diffraction and optical transparency, with feature size down to 10-100 nm. Soft lithography techniques is termed as 'multilayer soft lithography' and developed by Quake et al.<sup>59</sup> in 2000. Briefly, multilayer structures were formed by bonding PDMS layers from separated cast in a micromachining mold. Since each layer has excess of one of the components, the reactive molecules remained at the interface form permanent bonding after further curing. They used such technique for development of microfluidic large-scale integration chips that contain plumbing networks with thousands of micromechanical PDMS valves and hundreds of individually addressable chambers. Their chips can be used to construct the microfluidic analog of a comparator array and a microfluidic memory storage device similar to the behavior of random-access memory.

PDMS microfluidics have great potential to be biomedical applications which only require small amounts of sample, routine operation by untrained personnel and low cost<sup>65</sup>. One of such examples was developed on a simple, inexpensive PDMS microfluidic diagnostic device, which performs sandwich immunoassays for medicine and biological studies<sup>12, 63</sup>. Screws are used in the device as virtual valves to on and off fluids. The low-cost on soft lithography microfabrication and raw materials makes this device great potential for portable healthcare delivery and monitoring. PDMS microfluidics can be used for reagent mixing in microscale channel<sup>66</sup>. The challenge for flow mixing in a small dimension is mainly due to the difficult liquid turbulence inside chip. By use of PDMS as microfluidics substrate, a topological structure can be fabricated to exploit the laminarity of the flow to repeatedly fold the flow and double the lateral concentration gradient in a compact chip. Two different solutions are contained in a T-junction, and fluid flow is repeatedly split, rotated, and merged<sup>67</sup>. The chip design was obtained by a rapid-prototyping master mold, and results showed that effective mixing can be achieved on short length scales.

PDMS microfluidics has applied to a variety of applications such as cell sorting, DNA sizing and sorting. DNA sequence is successfully performed in PDMS devices including sample preparation and electrophoresis analysis<sup>14</sup>. PDMS has substantial advantages over glass or silicon dioxide substrates, since these latter materials were adhesive for the cells of interest. In addition, Chou et al.<sup>68</sup> developed a PDMS device for the sizing and sorting of restriction fragments of DNA based on single DNA molecule detection. The device sizes DNA on the basis of fluorescence intensity in which the DNA was labeled with fluorescence dye.

PDMS device can be easily fabricated by non-covalent bonding or plasma treated permanent bonding after replica by molding. The PDMS microfluidics for capillary electrophoresis was developed by Effenhauser et al.<sup>69</sup> in 1997. They used replica molding to obtain PDMS device and bonded reversibly the device with a flat piece of PDMS. The performance of PDMS CE is not ideal on unmodified surface, especially for proteins/peptides analysis, due to hydrophobicity of the unmodified PDMS surface. Later, Whitesides et al. developed PDMS microfluidics device by a rapid prototyping and irreversible bonding through plasma

oxidation<sup>19</sup>. Different PDMS devices were developed to demonstrate separation performance of fluorescently labeled amino acids and proteins using capillary zone electrophoresis (CZE) and gel electrophoresis (GE).

One-dimensional sodium dodecyl sulfate (SDS) capillary gel electrophoresis (CGE) can be also performed in PDMS microfluidics due to its versatile surface chemistry. PDMS surface is treated by UV-Ozone so that it could immobilize other hydrophilic molecules to prevent electroosmotic flow and protein/peptide non-specific binding. For complex cell lysate analysis, isoelectric focusing (IEF) can be interfaced with SDS-CGE as the first dimension separation. What makes PDMS special for IEF-SDS/CGE is because of conventional procedures for fabricating 3-D microfluidic channels<sup>70</sup>, and the facility with which PDMS-based devices can be readily assembled and disassembled. For example, after IEF separation, the PDMS was disassembled and connected with a 3-D channel for SDS/CGE. Recent development on 2-D IEF-SDS/CGE showed that other thermoplastic would be better substrate of choice for integrated 2-D complex cell lysate analysis<sup>71,72</sup>.

The design of elastomer microfluidics can be made based on these studies<sup>71-73</sup>. The electrokinetic injection of defined sample plugs within single dimension microfluidic systems has been extensively studied, with the most widely used injector configurations including the cross, double-T, and triple-T topologies<sup>74,75</sup>, and extended configurations employing continuous sample injection leveraging flow switching techniques. Floating injection and pinched-injection methods<sup>76,77</sup> have been employed in simple cross-injectors for the controlled definition of small sample plugs, while double- and triple-T designs are generally employed for the introduction of larger sample volumes. Sample leakage<sup>78</sup> was observed in a 2-D device during sample injection which was the central issue for separation performance as shown in Figure 4. After the desired sample plug has been transferred to the separation channel, additional samples enter the injection region due to diffusion and fringing of the electrical field during the electrokinetic transfer process. The excess sample tailing degrades separation performance. To solve this issue, backbiasing is a commonly used to eliminate sample leakage. Practically, bias voltages can be applied to sample inlet and waste reservoirs, electrokinetically pulling back excess sample from the injection zone. The effective of this approach depended on the accurate selection of backbiasing bias. This requires characterization of device geometry, medium in device, and buffer resistivity. A few groups<sup>49,72,79</sup> have proposed 2-D chip designs consisting of an array of second dimension separation channels aligned with an identical number of injection channels on the opposite side of the first dimension microchannel, a more efficient design for spatially multiplexed 2-D separation chips is shown in Figure 4 (a). The design consists of a single first dimension separation channel intersected by multiple second dimension separation channels on one side, and sample injection channels on the opposite side, with the injection channels staggered with respect to the separation channels to ensure complete and simultaneous sampling of species separated in the first dimension channel. In this staggered design, the parallel second dimension microchannels may be regarded as an array of double-T injectors operating in parallel. However, unlike the single-channel case, the double-T injectors are not electrically isolated in the multidimensional system.

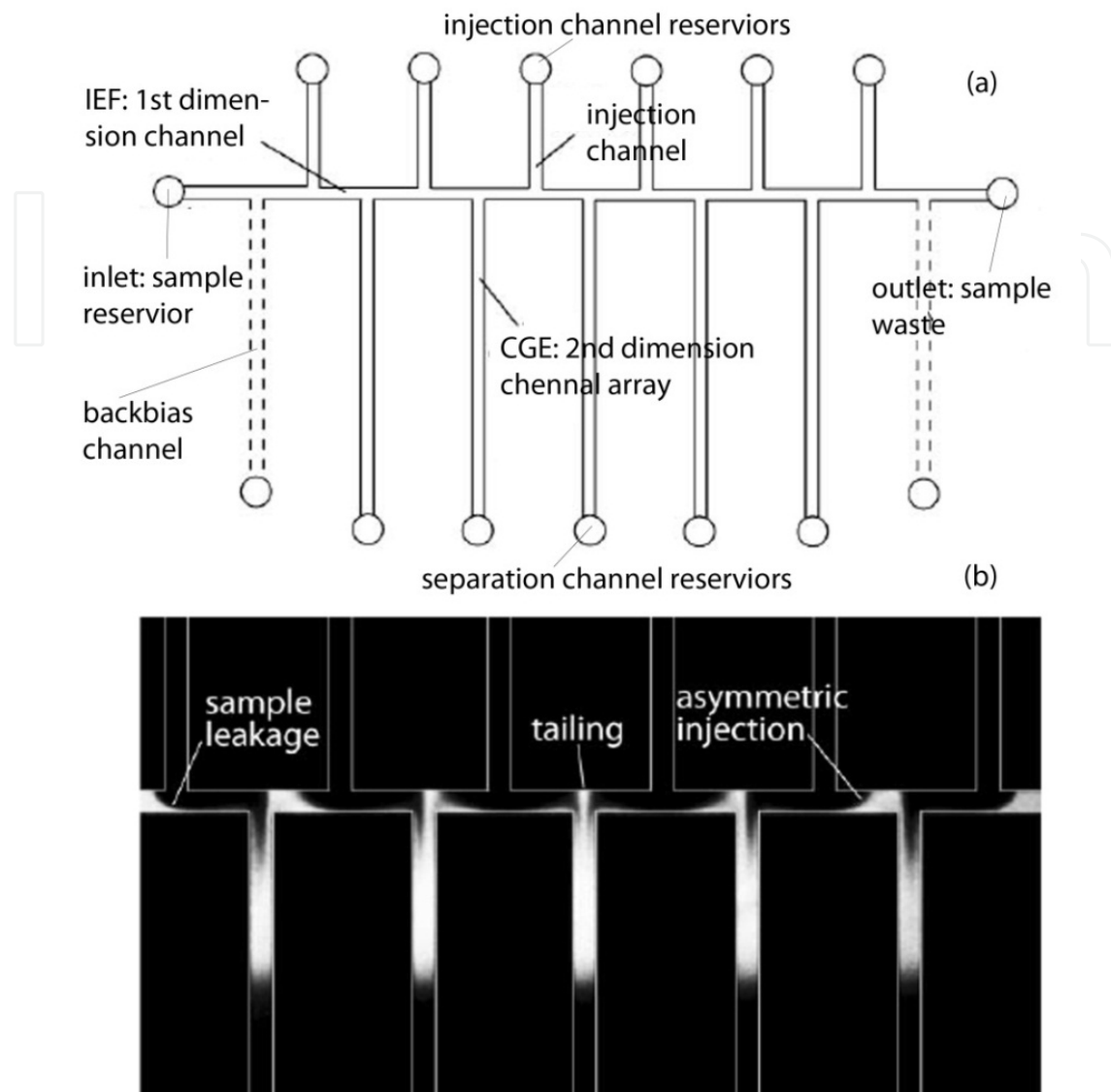


**Figure 4.** Schematic diagram of two-dimensional capillary electrophoresis microfluidics design with (a) simplified device of a spatially-multiplexed separation platform with five second dimension microchannels, and (b) image during the sample transfer process using a fabricated chip without backbias channels. Reprint and permission from <sup>71</sup>

This interconnected design can result in significant variations in performance between the different injectors, as depicted in Figure 4 (b). In this image, the sample within the first dimension channel is being electrokinetically transferred into the second dimension channel array by applying a uniform bias voltage in the injection channel reservoirs while grounding the second dimension reservoirs. Three main features are evident in this injection process. The substantial tailing of sample occurs at the head of each second dimension channel, resulting in sample dispersion during transfer; in all but the center second dimension channel, the injection is highly asymmetric, reflecting a non-uniform electric field distribution within the first dimension channel; sample from the outermost regions of the first dimension channel

continually leaks into the second dimension array due to a combination of diffusion and electric field fringing, leading to additional tailing which can continue long after sample from the center region of the first dimension channel has been fully transferred separation devices .

The solution for unsymmetrical injection and tailing was proposed by adding backbias channels parallel to the separation channels as shown in Figure 4 (b) <sup>70</sup>. Analytical calculation indicated that two-fold of resistance in the backbias channel generated uniform current and potential distribution in the 2-D channel network, not only in 1-D channel, but also injection and separation channels. Additionally, the angled 1-D channel can level the electric field distribution in the local region of T intersection. As a result, the angled 1-D channel substantially reduced sample tailing with negligible effect on the first dimension separation. These design perspectives have been used for complex biological sample analysis.

Use of PDMS for liquid chromatography has been limited largely due to its low bonding strength <sup>80</sup> and high gas/liquid permeability <sup>81</sup>. It was reported to fabricate column in a device using PDMS <sup>82-84</sup>. Since PDMS is inexpensive and thus it can be fabricated as a disposable column, it can be used as a stationary phase in liquid chromatography columns. The siloxane monomer was added into a molding to formation of desired features. The featured PDMS was reversibly sealed with cover PDMS by placing the molded chip in contact with cover PDMS, or irreversibly sealed by plasma oxidation. The PDMS chip was treated with silanes to minimize sample non-specific absorption. In general, PDMS is not the good materials of choice for high performance liquid chromatography. In such instance, other thermoplastics such as polyimide (PI) <sup>85</sup>, fused silica capillary <sup>75</sup>, cyclic olefin copolymer (CoC) <sup>86</sup>, are recommended.

Droplets formed by mixing one fluid in another or emulsions are very useful in a wide range of applications including personal care products, foods, microbiology, cell biology, and drug delivery vehicles <sup>87, 88</sup>. It has been recognized that a successful droplet device for applications is able to control over size and distribution in microscale and nanoscale emulsions <sup>88</sup>. Droplet formation can be obtained by either turbulence to break apart an immiscible mixture or continuous flow. PDMS devices for micro-droplet formation are fabricated by soft lithography in a molding. The native PDMS surface is usually hydrophobic and excellent surface for water-in-oil emulsions. The hydrophobic PDMS surface ensures that the oil droplets encapsulation of water phase inside without being contacted the PDMS channel walls <sup>89, 90</sup>; while hydrophilic PDMS surface can be used for oil-in-water droplets and biological sample analysis <sup>91, 92</sup>. Several surface modifications have been reported by the sequential layer-by-layer deposition of polyelectrolytes yielding hydrophilic microchannels. Others used oxygen-plasma and oxygen-C2F6 to modify PDMS surface in order to enhance hydrophilicity and reduce channel electroosmotic flow (EOF). Alternatively, use of chemical modification, e.g., 2-hydroxyethyl methacrylate (HEMA), can permanently enhance PDMS hydrophilicity <sup>91</sup>. In layer-by-layer (LbL) surface modification approach, segments of sodium chloride, poly(allylamine hydrochloride), and poly(sodium 4-styrenesulfonate) solutions are separated by air plugs and loaded into a piece of tubing and sequentially flushed through the channel at a constant flow rate. This LbL modification provides long storage time up to 5 months without noticeable behavior change of droplet formation. The LbL modified PDMS device can be used for water-oil-water double emulsion system for applications such as pharmaceutical compound delivery.

An interesting PDMS device for static microdroplet arrays is fabricated to droplet trapping, incubation, and release of enzymatic and cell-based assays<sup>93</sup>. They simply used a single-layered PDMS microfluidic structure. The aqueous droplets are trapped en masse and optically monitored for extended periods of time. The array droplet approach is used to characterize droplet shrinkage, aggregation of encapsulated biological cells and enzymatic reactions. On the other hand, to optimize the droplet formation, a design which use feedback control loop is developed<sup>88</sup>. They successfully demonstrated that the closed loop control system with negative feedback can produce the required droplet size with minimal noise and no systematic steady state error. This close-loop design is utilized for a number of applications, including micro-chemistry and emulsion production.

## 5. Outlook of elastomer application

The application of elastomer is being continuously exploited. The future of elastomer is closely related to the specific requirement on applications. One of the hot topics is development of nano- and microfluidics for assisted reproductive technologies<sup>94</sup>. For example, the studies have demonstrated that thickness of PDMS layers at 100  $\mu\text{m}$  in chips produced significantly fewer embryos due to drastically shift in osmolality of embryo-culture media. It could be the solution by development of a hybrid membrane consisting of PDMS-parylene-PDMS for maintaining a stable cell growth environment. Therefore, investigation of new type of PDMS materials or hybrid PDMS can provide means for such applications.

Due to the low bonding strength, PDMS has seldom used for high performance liquid chromatography application (HPLC). The HPLC can be directly interfaced with detection system such as electrospray ionization or mass spectrometry. As a result, it becomes research of interest to synthesize PDMS which has strong bonding strength (via covalent bond) and low permeability, while PDMS optical transparency and elasticity are largely remained. In summary, PDMS is becoming more and more popular as the materials of choice for biological analysis due to its good physical, mechanical, and chemical properties, as well as its excellent biocompatibility.

A thermoplastic rubber material has recently been developed that can completely mend itself when the fracture interfaces are rejoined and left to heal for a moderate time<sup>95</sup>. This "smart" rubber is easy to synthesize and displays excellent mechanical properties. This material could be used for microelectronics, microfluidics and biology system.

### Author details

Shuang (Jake) Yang\*

*Department of Pathology, Johns Hopkins University, Baltimore, USA*

Shuang (Jake) Yang and Kunqiang Jiang

*Department of Mechanical Engineering, University of Maryland, USA*

*Department of Chemistry and Biochemistry, University of Maryland, USA*

---

\* Corresponding Author

## 6. References

- [1] Legge, N.R. Thermoplastic elastomers. 60, 83 (1987).
- [2] Eisenbach, C., Baumgartner, M. & Gunter, C. Advances in Elastomers and Rubber Elasticity. 51 (1986).
- [3] Markham, R.L. & Mueller, W.J. (Google Patents, 1986).
- [4] Massey, L.K. Permeability Properties of Plastics and Elastomers: A Guide to Packaging and Barrier Materials, Edn. 2<sup>nd</sup>. (Plastics Design Library / William Andrew Publishing, Norwich, NY; 2002).
- [5] Simmons, S., Shah, M., Mackevich, J. & Chang, R.J. Polymer outdoor insulating materials Part III-silicone elastomer considerations. 13, 8 (19978).
- [6] Lin, Y.H., Kang, S.W. & Wu, T.Y. Fabrication of polydimethylsiloxane (PDMS) pulsating heat pipe. 29, 573-580 (2009).
- [7] Jafari, S.H. & Gupta, A.K. Impact strength and dynamic mechanical properties correlation in elastomer-modified polypropylene. *J Appl Polym Sci* 78, 962-971 (2000).
- [8] Yang, S., Zhang, Y.W. & Zeng, K.Y. Analysis of nanoindentation creep for polymeric materials. *J Appl Phys* 95, 3655-3666 (2004).
- [9] White, C.C., Vanlandingham, M.R., Drzal, P.L., Chang, N.K. & Chang, S.H. Viscoelastic characterization of polymers using instrumented indentation. II. Dynamic testing. *J Polym Sci Pol Phys* 43, 1812-1824 (2005).
- [10] Jancar, J., Dianselmo, A., Dibenedetto, A.T. & Kucera, J. Failure Mechanics in Elastomer Toughened Polypropylene. *Polymer* 34, 1684-1694 (1993).
- [11] Toepke, M.W. & Beebe, D.J. PDMS absorption of small molecules and consequences in microfluidic applications. 6, 1484-1486 (2006).
- [12] Eteshola, E. & Leckband, D. Development and characterization of an ELISA assay in PDMS microfluidic channels. 72, 129-133 (2001).
- [13] Martin, R.S., Gawron, A.J., Lunte, S.M. & Henry, C.S. Dual-electrode electrochemical detection for poly (dimethylsiloxane)-fabricated capillary electrophoresis microchips. 72, 3196-3202 (2000).
- [14] Paegel, B.M., Blazej, R.G. & Mathies, R.A. Microfluidic devices for DNA sequencing: sample preparation and electrophoretic analysis. 14, 42-50 (2003).
- [15] Scott, N. An area modulus of elasticity: definition and properties. 58, 269-275 (2000).
- [16] Yang, S., Wu, J. & Pecht, M.G. Reliability Assessment of Land Grid Array Sockets Subjected to Mixed Flowing Gas Environment. *Ieee T Reliab* 58, 634-640 (2009).
- [17] Liu, W. & Pecht, M. IC component sockets. (Wiley-Blackwell, 2004).
- [18] Lee, J.N., Park, C. & Whitesides, G.M. Solvent compatibility of poly (dimethylsiloxane)-based microfluidic devices. 75, 6544-6554 (2003).
- [19] McDonald, J.C. et al. Fabrication of microfluidic systems in poly(dimethylsiloxane). *Electrophoresis* 21, 27-40 (2000).
- [20] Eddings, M.A. & Gale, B.K. A PDMS-based gas permeation pump for on-chip fluid handling in microfluidic devices. 16, 2396 (2006).
- [21] Mark, J.E. Some unusual elastomers and experiments on rubberlike elasticity. *Prog Polym Sci* 28, 1205-1221 (2003).

- [22] Lawn, B. & Wilshaw, R. Indentation Fracture - Principles and Applications. *J Mater Sci* 10, 1049-1081 (1975).
- [23] Oliver, W.C. & Pharr, G.M. An Improved Technique for Determining Hardness and Elastic-Modulus Using Load and Displacement Sensing Indentation Experiments. *J Mater Res* 7, 1564-1583 (1992).
- [24] Carrillo, F. et al. Nanoindentation of polydimethylsiloxane elastomers: Effect of crosslinking, work of adhesion, and fluid environment on elastic modulus. *J Mater Res* 20, 2820-2830 (2005).
- [25] Bao, T., Morrison, P.W. & Woyczynski, W. AFM nanoindentation as a method to determine microhardness of hard thin films. *Mater Res Soc Symp P* 517, 395-400 (1998).
- [26] Oyen, M.L. Sensitivity of polymer nanoindentation creep measurements to experimental variables. 55, 3633-3639 (2007).
- [27] Mata, A., Fleischman, A.J. & Roy, S. Characterization of polydimethylsiloxane (PDMS) properties for biomedical micro/nanosystems. 7, 281-293 (2005).
- [28] Singh, A., Freeman, B.D. & Pinnau, I. Pure and mixed gas acetone/nitrogen permeation properties of polydimethylsiloxane [PDMS]. *J Polym Sci Pol Phys* 36, 289-301 (1998).
- [29] Kurian, P. et al. Synthesis, permeability and biocompatibility of tricomponent membranes containing polyethylene glycol, polydimethylsiloxane and poly(pentamethylcyclopentasiloxane) domains. *Biomaterials* 24, 3493-3503 (2003).
- [30] Pinnau, I. & He, Z.J. Pure- and mixed-gas permeation properties of polydimethylsiloxane for hydrocarbon/methane and hydrocarbon/hydrogen separation. *J Membrane Sci* 244, 227-233 (2004).
- [31] Leclerc, E., Sakai, Y. & Fujii, T. Microfluidic PDMS (polydimethylsiloxane) bioreactor for large-scale culture of hepatocytes. 20, 750-755 (2004).
- [32] Abate, A.R., Lee, D., Do, T., Holtze, C. & Weitz, D.A. Glass coating for PDMS microfluidic channels by sol-gel methods. 8, 516-518 (2008).
- [33] Ghosal, K. & Freeman, B.D. Gas separation using polymer membranes: an overview. 5, 673-697 (1994).
- [34] Shiku, H. et al. Oxygen permeability of surface-modified poly(dimethylsiloxane) characterized by scanning electrochemical microscopy. *Chem Lett* 35, 234-235 (2006).
- [35] Leclerc, E., Sakai, Y. & Fujii, T. Cell culture in 3-dimensional microfluidic structure of PDMS (polydimethylsiloxane). *Biomed Microdevices* 5, 109-114 (2003).
- [36] Tummala, R.R., Rymaszewski, E.J. & Klopfenstein, A.G. *Microelectronics Packaging Handbook*. (Kluwer Academic Publishers Group, Norwell, MA; 1997).
- [37] Kim, J., Chaudhury, M.K. & Owen, M.J. Hydrophobicity loss and recovery of silicone HV insulation. *Ieee T Dielect El In* 6, 695-702 (1999).
- [38] Liu, H.P., Cash, G., Birtwhistle, D. & George, G. Characterization of a severely degraded silicone elastomer HV insulator - an aid to development of lifetime assessment techniques. *Ieee T Dielect El In* 12, 478-486 (2005).
- [39] Park, J., Kim, H.S. & Han, A. Micropatterning of poly(dimethylsiloxane) using a photoresist lift-off technique for selective electrical insulation of microelectrode arrays. *J Micromech Microeng* 19 (2009).

- [40] Nam, Y., Musick, K. & Wheeler, B.C. Application of a PDMS microstencil as a replaceable insulator toward a single-use planar microelectrode array. *Biomed Microdevices* 8, 375-381 (2006).
- [41] Tong, X.C. *Advanced Materials for Thermal Management of Electronic Packaging*, Edn. 1<sup>st</sup>. (Springer Science & Business Media, LLC, New York; 2010).
- [42] Lee, K.I. & Jopson, H. Electrically Conductive Thermoplastic Elastomer Polyacetylene Blends. *Polym Bull* 10, 105-108 (1983).
- [43] Pelrine, R., Kornbluh, R., Pei, Q.B. & Joseph, J. High-speed electrically actuated elastomers with strain greater than 100%. *Science* 287, 836-839 (2000).
- [44] Faez, R., Schuster, R.H. & De Paoli, M.A. A conductive elastomer based on EPDM and polyaniline. II. Effect of the crosslinking method. *Eur Polym J* 38, 2459-2463 (2002).
- [45] Yang, S., Wu, J., Tsai, D. & Pecht, M.G. Contact resistance estimation for time-dependent silicone elastomer matrix of land grid array socket. *Ieee T Compon Pack T* 30, 81-85 (2007).
- [46] Jin, S. et al. New, Z-Direction Anisotropically Conductive Composites. *J Appl Phys* 64, 6008-6010 (1988).
- [47] Jin, S., Tiefel, T.H., Wolfe, R., Sherwood, R.C. & Mottine, J.J. Optically Transparent, Electrically Conductive Composite Medium. *Science* 255, 446-448 (1992).
- [48] Ausanio, G. et al. Giant resistivity change induced by strain in a composite of conducting particles in an elastomer matrix. *Sensor Actuat a-Phys* 127, 56-62 (2006).
- [49] Chen, L.H., Jin, S. & Tiefel, T.H. Tactile Shear Sensing Using Anisotropically Conductive Polymer. *Appl Phys Lett* 62, 2440-2442 (1993).
- [50] Yang, S., Wu, J. & Pecht, M. Electrochemical migration of land grid array sockets under highly accelerated stress conditions. 238-244 (2005).
- [51] Yang, S., Wu, J. & Christou, A. Initial stage of silver electrochemical migration degradation. *Microelectron Reliab* 46, 1915-1921 (2006).
- [52] Yang, S.A. & Christou, A. Failure model for silver electrochemical migration. *Ieee T Device Mat Re* 7, 188-196 (2007).
- [53] Liu, W.F., Pecht, M.G. & Xie, J.S. Fundamental reliability issues associated with a commercial particle-in-elastomer interconnection system. *Ieee T Compon Pack T* 24, 520-525 (2001).
- [54] Krumbein, S.J. Metallic Electromigration Phenomena. *Ieee T Compon Hybr* 11, 5-15 (1988).
- [55] Zamanzadeh, M., Meilink, S.L., Warren, G.W., Wynblatt, P. & Yan, B. Electrochemical Examination of Dendritic Growth on Electronic Devices in Hcl Electrolytes. *Corrosion* 46, 665-671 (1990).
- [56] Ruschau, G.R., Yoshikawa, S. & Newnham, R.E. Resistivities of Conductive Composites. *J Appl Phys* 72, 953-959 (1992).
- [57] Brunauer, S., Emmett, P.H. & Teller, E. Adsorption of gases in multimolecular layers. *J Am Chem Soc* 60, 309-319 (1938).
- [58] Findley, W.N., Lai, J.S. & Onaran, K. *Creep and Relaxation of Nonlinear Viscoelastic Materials*. (Dover, New York; 1975).

- [59] Unger, M.A., Chou, H.P., Thorsen, T., Scherer, A. & Quake, S.R. Monolithic microfabricated valves and pumps by multilayer soft lithography. *Science* 288, 113-116 (2000).
- [60] Melin, J. & Quake, S.R. Microfluidic large-scale integration: The evolution of design rules for biological automation. *Annu Rev Bioph Biom* 36, 213-231 (2007).
- [61] Erickson, D. & Li, D.Q. Integrated microfluidic devices. *Anal Chim Acta* 507, 11-26 (2004).
- [62] de Mello, A. On-chip chromatography: the last twenty years. *Lab Chip* 2, 48n-54n (2002).
- [63] Xia, Y.N. & Whitesides, G.M. Soft lithography. *Angew Chem Int Edit* 37, 551-575 (1998).
- [64] Levenson, M.D., Viswanathan, N. & Simpson, R.A. Improving resolution in photolithography with a phase-shifting mask. 29, 1828-1836 (1982).
- [65] Paguirigan, A.L. & Beebe, D.J. Microfluidics meet cell biology: bridging the gap by validation and application of microscale techniques for cell biological assays. 30, 811-821 (2008).
- [66] Song, H. & Ismagilov, R.F. Millisecond kinetics on a microfluidic chip using nanoliters of reagents. 125, 14613-14619 (2003).
- [67] Chen, H. & Meiners, J.C. Topologic mixing on a microfluidic chip. 84, 2193 (2004).
- [68] Chou, H.P., Spence, C., Scherer, A. & Quake, S. A microfabricated device for sizing and sorting DNA molecules. 96, 11 (1999).
- [69] Effenhauser, C.S., Bruin, G.J.M., Paulus, A. & Ehrat, M. Integrated capillary electrophoresis on flexible silicone microdevices: analysis of DNA restriction fragments and detection of single DNA molecules on microchips. 69, 3451-3457 (1997).
- [70] Jo, B.H., Van Lerberghe, L.M., Motsegood, K.M. & Beebe, D.J. Three-dimensional micro-channel fabrication in polydimethylsiloxane (PDMS) elastomer. 9, 76-81 (2000).
- [71] Yang, S., Liu, J. & DeVoe, D.L. Optimization of sample transfer in two-dimensional microfluidic separation systems. *Lab Chip* 8, 1145-1152 (2008).
- [72] Yang, S., Liu, J.K., Lee, C.S. & Devoe, D.L. Microfluidic 2-D PAGE using multifunctional in situ polyacrylamide gels and discontinuous buffers. *Lab Chip* 9, 592-599 (2009).
- [73] Liu, J.K., Yang, S., Lee, C.S. & Devoe, D.L. Polyacrylamide gel plugs enabling 2-D microfluidic protein separations via isoelectric focusing and multiplexed sodium dodecyl sulfate gel electrophoresis. *Electrophoresis* 29, 2241-2250 (2008).
- [74] Fu, L.M., Yang, R.J., Lee, G.B. & Liu, H.H. Electrokinetic injection techniques in microfluidic chips. 74, 5084-5091 (2002).
- [75] Blas, M., Delaunay, N. & Rocca, J.L. Electrokinetic-based injection modes for separative microsystems. 29, 20-32 (2008).
- [76] Hirokawa, T., Takayama, Y., Arai, A. & Xu, Z. Study of a novel sample injection method (floating electrokinetic supercharging) for high-performance microchip electrophoresis of DNA fragments. 29, 1829-1835 (2008).
- [77] Zhang, L., Yin, X. & Fang, Z. Negative pressure pinched sample injection for microchip-based electrophoresis. 6, 258-264 (2006).
- [78] Duffy, D.C., McDonald, J.C., Schueller, O.J.A. & Whitesides, G.M. Rapid prototyping of microfluidic systems in poly (dimethylsiloxane). 70, 4974-4984 (1998).

- [79] Li, Y., Buch, J.S., Rosenberger, F., DeVoe, D.L. & Lee, C.S. Integration of isoelectric focusing with parallel sodium dodecyl sulfate gel electrophoresis for multidimensional protein separations in a plastic microfluidic network. 76, 742-748 (2004).
- [80] Gent, A. & Tobias, R. Effect of interfacial bonding on the strength of adhesion of elastomers. III. Interlinking by molecular entanglements. 22, 1483-1490 (1984).
- [81] Kuncová-Kallio, J. & Kallio, P.J. 2486-2489 (IEEE, 2006).
- [82] Weng, X., Chon, C.H., Jiang, H. & Li, D. Rapid detection of formaldehyde concentration in food on a polydimethylsiloxane (PDMS) microfluidic chip. 114, 1079-1082 (2009).
- [83] Slentz, B.E., Penner, N.A., Lugowska, E. & Regnier, F. Nanoliter capillary electrochromatography columns based on collocated monolithic support structures molded in poly (dimethyl siloxane). 22, 3736-3743 (2001).
- [84] Ocvirk, G. et al. Electrokinetic control of fluid flow in native poly (dimethylsiloxane) capillary electrophoresis devices. 21, 107-115 (2000).
- [85] Levkin, P.A. et al. Monolithic porous polymer stationary phases in polyimide chips for the fast high-performance liquid chromatography separation of proteins and peptides. 1200, 55-61 (2008).
- [86] Mair, D.A., Geiger, E., Pisano, A.P., Fréchet, J.M.J. & Svec, F. Injection molded microfluidic chips featuring integrated interconnects. 6, 1346-1354 (2006).
- [87] Anna, S.L., Bontoux, N. & Stone, H.A. Formation of dispersions using “flow focusing” in microchannels. 82, 364 (2003).
- [88] Miller, E., Rotea, M. & Rothstein, J.P. Microfluidic device incorporating closed loop feedback control for uniform and tunable production of micro-droplets. 10, 1293-1301 (2010).
- [89] Link, D.R. et al. Electric control of droplets in microfluidic devices. 45, 2556-2560 (2006).
- [90] Fujii, T. PDMS-based microfluidic devices for biomedical applications. 61, 907-914 (2002).
- [91] Bodas, D. & Khan-Malek, C. Formation of more stable hydrophilic surfaces of PDMS by plasma and chemical treatments. 83, 1277-1279 (2006).
- [92] Bauer, W.A.C., Fischlechner, M., Abell, C. & Huck, W.T.S. Hydrophilic PDMS microchannels for high-throughput formation of oil-in-water microdroplets and water-in-oil-in-water double emulsions. 10, 1814-1819 (2010).
- [93] Huebner, A. et al. Static microdroplet arrays: a microfluidic device for droplet trapping, incubation and release for enzymatic and cell-based assays. 9, 692-698 (2009).
- [94] Beebe, D., Wheeler, M., Zeringue, H., Walters, E. & Raty, S. Microfluidic technology for assisted reproduction. 57, 125-135 (2002).
- [95] Wietor, J.L. & Sijbesma, R.P. A Self-Healing Elastomer. 47, 8161-8163 (2008).